of the winds at the cloudtop level, confirmed and refined by a variety of ground-based and spacecraft observations, was reported by C. Boyer and H. Camichel [*Ann. Astrophys.* **24**, 531 (1961)].
9. R. W. Carlson *et al.*, *Science* **253**, 1541 (1991).
10. D. Crisp *et al.*, *ibid.*, p. 1538.
11. L. W. Esposito *et al.*, *J. Geophys. Res.* **93**, 5267 (1988); C. Y. Na, L. W. Esposito, T. E. Skinner, *ibid.* **95**, 74 (1990); L. W. Esposito, personal communication.
12. G. M. Keating *et al.*, *Adv. Space Res.* **5**, 117 (1985).
13. D. J. Diner, J. Apt, L. S. Elson, *Icarus* **52**, 301 (1982), and references therein.
14. J. T. Schofield and F. W. Taylor, *Q. J. R. Meterol. Soc.* **109**, 57 (1983).
15. Assuming optical constants given by K. F. Palmer and D. Williams [*Appl. Opt.* **14**, 208 (1975)].
16. G.S.O., J. C., and T.Z.M. were visiting astronomers at the Infrared Telescope Facility (IRTF), which is operated by the University of Hawaii under contract to NASA. We thank the staff and management of the IRTF for their support, particularly site superintendent R. Koehler, and we thank IRTF Division Chief R. Joseph for his scheduling of these observations. NASA sponsored the work performed at the Jet Propulsion Laboratory (JPL), California Institute of Technology, and the National Research Council of Canada sponsored work performed at York University. G.S.O. and T.Z.M. particularly acknowledge support from the Galileo Project. We also appreciate the advice of D. J. Diner, J. V. Martonchik, and J. T. Schofield at various points in this work. N. Ha also provided essential data reduction support during his tenure at JPL as a Caltech Summer Undergraduate Research Fellow.

26 April 1991; accepted 18 July 1991

# Ground-Based Near-Infrared Imaging Observations of Venus During the Galileo Encounter

D. CRISP, S. MCMULDROCH, S. K. STEPHENS, W. M. SINTON,*
B. RAGENT, K.-W. HODAPP, R. G. PROBST, L. R. DOYLE,
D. A. ALLEN, J. ELIAS

**Near-infrared images of Venus, obtained from a global network of ground-based observatories during January and February 1990, document the morphology and motions of the night-side near-infrared markings before, during, and after the Galileo Venus encounter. A dark cloud extended halfway around the planet at low latitudes ($< \pm 40°$) and persisted throughout the observing program. It had a rotation period of 5.5 ± 0.15 days. The remainder of this latitude band was characterized by small-scale (400 to 1000 kilometers) dark and bright markings with rotation periods of 7.4 ± 1 days. The different rotation periods for the large dark cloud and the smaller markings suggests that they are produced at different altitudes. Mid-latitudes ($\pm 40°$ to 60°) were usually occupied by bright east-west bands. The highest observable latitudes ($\pm 60°$ to 70°) were always dark and featureless, indicating greater cloud opacity. Maps of the water vapor distribution show no evidence for large horizontal gradients in the lower atmosphere of Venus.**

IMAGES OF THE NIGHT SIDE OF VENUS taken at near-infrared (NIR) wavelengths (1 to 2.5 μm) reveal bright and dark markings that rotate from east to west with periods of about 6 days (*1, 2*). This infrared emission is produced by hot gases in the lower atmosphere (0 to 50 km). It is most intense at wavelengths near 1.74 and 2.3 μm, in the relatively transparent "spectral windows" between strongly absorbing $CO_2$ and $H_2O$ bands in the Venus atmosphere. The planet-wide sulfuric acid ($H_2SO_4$) clouds provide the primary source of opacity in these windows (*2–6*). Kamp *et al.* (*4, 5*) found that 10 to 20% differences in the optical depths of the clouds could account for the contrast between bright and dark markings. They also derived water vapor mixing ratios near 40 parts per million by volume (ppmv) below the cloud base (47 km). This is 1/2.5 to 1/5 of that inferred from Pioneer Venus and Venera entry-probe measurements (*7–9*). More recent NIR imaging and spectroscopic observations (*6, 10–12*) support these conclusions and place new constraints on the composition and dynamics of the lower Venus atmosphere.

The Galileo spacecraft's flyby of Venus on 10 February 1990 provided a novel opportunity to study the night-side NIR emission. The Galileo Near-Infrared Mapping Spectrometer (NIMS) acquired two high spatial resolution (25 to 50 km) maps of the Venus night side at 17 NIR wavelengths between 0.7 and 5.2 μm. This instrument also acquired complete NIR spectra of selected regions (*13*). To complement these spacecraft observations, a broad range of new NIR imaging and spectroscopic observations of Venus were acquired from a global network of ground-based observatories. The spectroscopic observations have been presented elsewhere (*6, 10–12, 14, 15*). The principal objective of the ground-based imaging program was to document the morphology and motions of the NIR markings before, during, and after the Galileo encounter. Thousands of NIR images were taken during the first week of January and during the first 2 weeks of February. These observing times were ideal for high-resolution imaging of the night side because Venus was near inferior conjunction (18 January 1990) with its night side facing Earth. Its angular size was about 50 arc sec, allowing about 50 resolution elements across the night side. Most images were taken in twilight or during the day because Venus was usually less than 30° from the sun. Images were collected almost continuously for 5- to 17-hour periods each observing day from sites that were widely separated in longitude (*16*). This high-resolution, long-duration time series allowed us to track a large number of distinct markings for periods ranging from 3 hours to 46 days (*17*).

The appearance of the Venus night side during January and February is shown in Figs. 1 and 2, respectively. These images were taken in the 2.3-μm spectral window where the NIR markings usually have the highest contrast. Low latitudes ($\pm 40°$) were characterized by a persistent large-scale (zonal wave number 1) pattern that moved from east to west (right to left in Figs. 2 and 3). The spatial extent of the bright and dark components of this pattern is more obvious in Fig. 3, A and B, where the imaging data from January and February, respectively, have been projected onto cylindrical latitude-longitude maps and combined to form global mosaics. A large, long-lived, dark patch that occupies this entire latitude range and covers about 180° of longitude was first seen on 1 to 2 January (Fig. 1, B and C), and again on 6 to 7 January (Fig. 1, F and G). Parts of it were also seen on 31 January, 5 February, and 10 to 12 February (Fig. 2, B and C and F through H). This dark patch, and a very similar feature seen in images taken in May and June 1988 (*2*), indicates the presence of increased $H_2SO_4$ cloud opacity (*4–6, 12, 15*).

Simulations of NIR spectra (*12, 15*) indicate that the darkest markings have 10 to 25%

D. Crisp, MS 169-237, Jet Propulsion Laboratory, California Institute of Technology, Pasadena, CA 91109; visiting astronomer, Palomar Observatory, California Institute of Technology, Pasadena, CA 91125.
S. McMuldroch and S. K. Stephens, Division of Geological and Planetary Sciences, California Institute of Technology, Pasadena, CA 91125; visiting astronomers, Las Campanas Observatory, Casilla 601, La Serena, Chile.
W. M. Sinton, Institute for Astronomy, University of Hawaii, Honolulu, HI 96822.
B. Ragent, San Jose State University Foundation, San Jose, CA 95192; visiting astronomer, University of Hawaii 0.6-m and 2.2-m telescopes at Mauna Kea Observatory, Mauna Kea, Hawaii.
K.-W. Hodapp, Institute for Astronomy, University of Hawaii, Honolulu, HI 96822.
R. G. Probst, Kitt Peak National Observatory, Tucson, AZ 85719.
L. R. Doyle, National Aeronautics and Space Administration (NASA) Ames Research Center, Moffett Field, CA 94035; visiting astronomer, Kitt Peak National Observatory, Tucson, AZ 85719.
D. A. Allen, Anglo-Australian Observatory, Post Office Box 296, Epping, New South Wales, Australia.
J. Elias, Cerro Tololo Inter-American Observatory, Casilla 603, La Serena, Chile.

*Present address: Lowell Observatory, Flagstaff, AZ 86001.

greater $H_2SO_4$ cloud optical depths than the brightest markings. Clouds in the optically thick dark markings absorb more of the upwelling thermal radiation from the hot lower atmosphere. Because of this, the dark markings experience more thermal radiative heating than the brighter markings. The horizontal heating contrasts associated with the long-lived, low-latitude bright-dark pattern should produce significant horizontal temperature variations within the clouds because the lifetime of this pattern exceeds the 1- to 2-week radiative relaxation times at these altitudes (*18*). This radiative mechanism could explain the anomalous 6.5 K offset between the vertical temperature profiles measured by the two Vega balloons (*19, 20*). Both balloons floated within the middle cloud at low latitudes, but they were separated by about 135° of longitude. Vega-1, which measured consistently higher temperatures than Vega-2 at the same pressure level, may have floated within a warmer dark marking, while Vega-2 sampled a cooler bright marking.

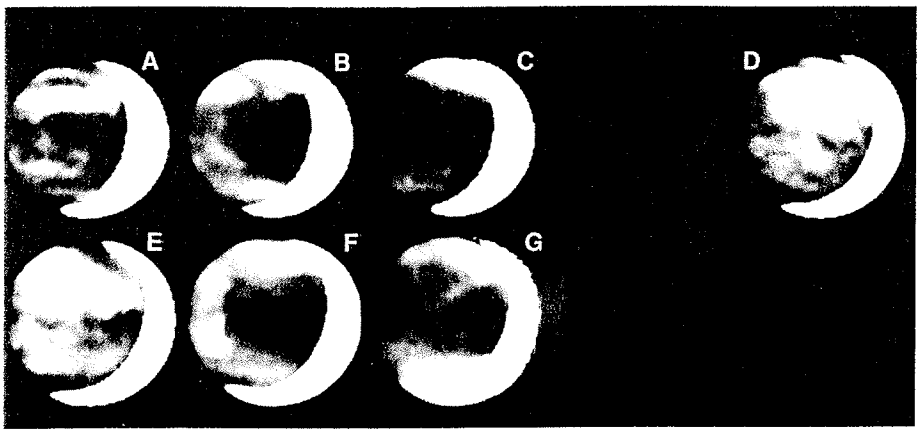


**Fig. 1.** One image of Venus at 2.36 μm is shown for each successful observing day before inferior conjunction. These images were arranged to illustrate the 5.5-day feature rotation period of the planetary-scale markings; (**A**) 31 December, 21:23 UT; (**B**) 1 January, 18:34 UT; (**C**) 2 January, 18:56 UT; (**D**) 5 January, 00:39 UT; (**E**) 5 January, 19:03 UT; (**F**) 6 January, 23:44 UT; (**G**) 7 January, 19:01 UT. A gap was left between images (C) and (D) because we have not yet completed the processing of the data from 3 January 1990. All images were obtained with the 58 × 62 element InSb NIR camera on the Kitt Peak National Observatory 1.3-m telescope. Images are oriented so that north (on the sky) is up and east (on the sky) is to the left. Before inferior conjunction, Venus was an afternoon-evening object, and the NIR markings moved from the bright crescent to the dark limb. We constructed each image by averaging up to 40 short exposures to increase the signal-to-noise ratio. We reduced the effects of scattered light from the bright sunlit crescent by subtracting out-of-band images (taken near 2.1 μm, where the night side emits little radiation) from each in-band (2.36 μm) image.

The large (2000 km) low-latitude bright spot centered near 16°N on 29 January (Fig. 2A) was seen again in images taken near midnight UT (universal time) on 9 February, just before the Galileo encounter, but it disappeared into the sunlit hemisphere before the first NIMS image was taken. It was centered on the opposite side of the planet from the large dark patch (Fig. 3B). This bright spot persisted for at least 11 days, but it dissipated before 15 February when it was expected to reappear on the night side. Its rotation period was 5.15 ± 0.1 days, indicating an average east-west velocity of 83 ± 2 m $s^{-1}$ at 16°N. No north-south motion was detected between 29 January and 10 February, which places an upper limit of 0.5 m $s^{-1}$ on its mean north-south velocity.

Bell *et al.* (*11, 12*) acquired a spectrum of this bright spot on 29 January and found that its intensity could be simulated by the removal of 60% of the mode 2′ (1.4-μm modal radius) and mode 3 (3.4-μm modal radius) particles from the middle (49 to 57 km) and lower (47 to 49 km) cloud decks. They also found that it was associated with the largest deep-atmosphere water vapor abundance ever measured from the ground. Their spectra from 29 January indicated water vapor

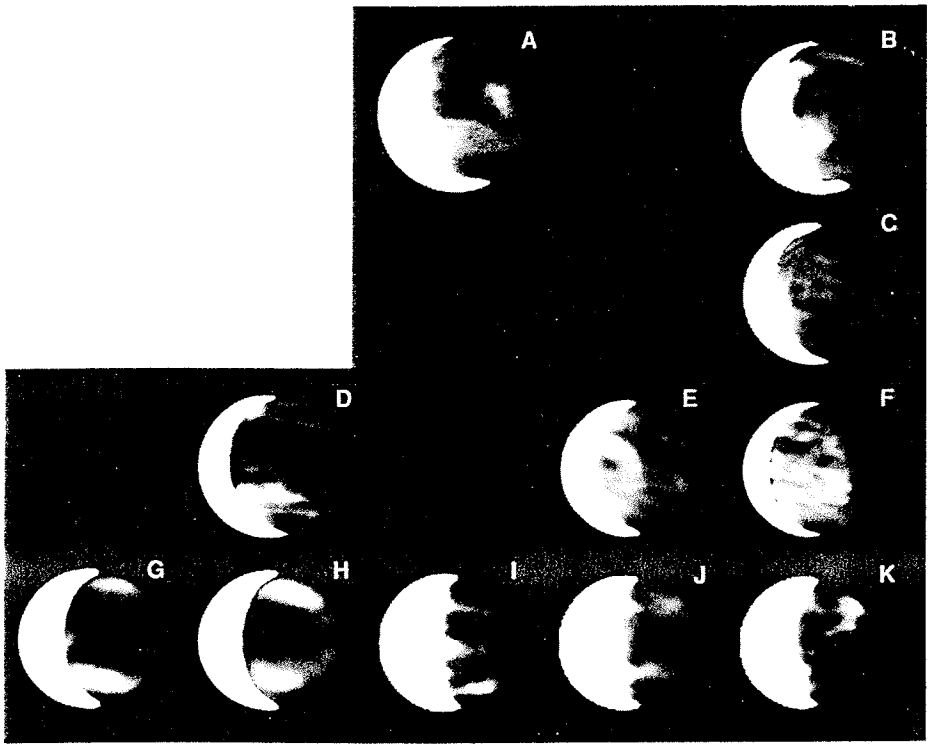


**Fig. 2.** One NIR image of Venus is shown from each successful day of the postconjunction period (29 January to 15 February 1990). Venus was in the morning sky, and the NIR features moved from the dark limb toward the bright crescent. Images were arranged to illustrate the 5.5-day period for the planetary-scale markings. Gaps indicate days with no data. (**A**) A K-band (2.2-μm) image taken with the University of Hawaii (UH) 256 × 256 element HgCdTe camera mounted on the Mauna Kea Observatory (MKO) 0.6-m telescope on 29 January, 17:10 UT. (**B**) Same as (A), but taken on 31 January, 17:51 UT. (**C**) Same as (A), but taken on 5 February, 17:09 UT. (**D**) A 2.36-μm image taken with the UH NICMOS camera on the UH 2.2-m telescope at MKO on 7 February, 19:38 UT. (**E**) Same as (D), but taken on 10 February, 00:50 UT, about 2 hours before the first Galileo NIMS image was taken. (**F**) Same as (D), but taken on 10 February, 17:01 UT. (**G**) A 2.38-μm image taken with the Palomar 256 × 256 element HgCdTe prime-focus camera on the Palomar 5-m telescope on 11 February, 14:13 UT. (**H**) Same as (G), but taken on 12 February, 13:58 UT. (I) A 2.36-μm image taken with the 128 × 128 element HgCdTe camera on the Las Campanas Observatory 1-m telescope on 13 February, 10:00 UT. (**J**) Same as (I), but taken on 14 February, 10:57 UT. (**K**) Same as (I), but taken on 15 February, 10:16 UT.

mixing ratios near 200 ppmv at pressures between 1 and 8 bars (30 and 50 km). This is 2.5 to 5 times as much water as other ground-based observers have reported (*5, 6, 15*), but it is comparable to that measured by the Pioneer Venus and Venera entry probes (*7, 8*). Bell *et al.* also took a spectrum of the dark marking just to the west of the bright spot and found much smaller water vapor mixing ratios (40 ppmv).

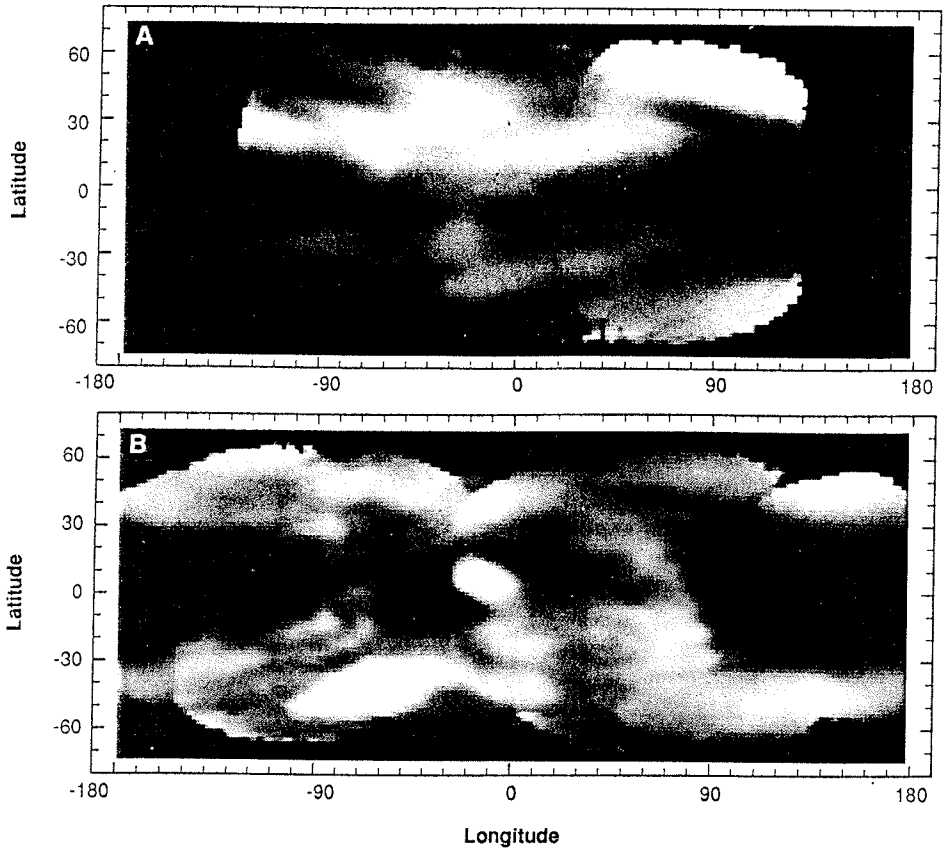


**Fig. 3.** Images of the Venus night side at 2.36 μm were projected onto a cylindrical latitude-longitude grid and then assembled into mosaics for (**A**) 31 December to 7 January and (**B**) 7 to 15 February. To register the images in longitude, a 5.5-day rotation period was assumed at all latitudes, and all longitude offsets were referenced to 00:00 UT on 10 February 1990. The longitude range seen by Galileo NIMS falls roughly between 0° and 90°. The alignment and overall similarity of the large-scale features in the January and February mosaics verify the 5.5-day period and show that the largest features have lifetimes that exceed 1 month. Small-scale features, like those that dominated the night side on 10 February, rarely persist for more than one rotation period.

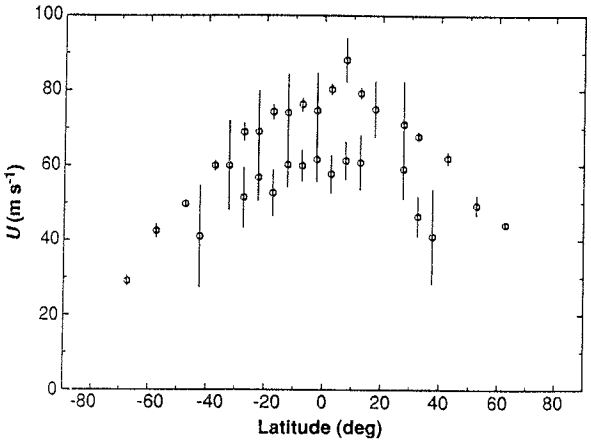


**Fig. 4.** All tracking results from January and February were combined to derive the velocities of NIR markings as a function of latitude. The error bars show 1 σ uncertainties for velocities measured in 5° latitude bins. These uncertainties are caused primarily by errors in the determination of the positions of distinct markings in different images. The largest uncertainties are contributed by the changes in the atmospheric seeing (blurring caused by Earth's atmosphere), digitization errors caused by the finite pixel sizes on the NIR detectors, foreshortening errors produced as features move close to the Venus limb, and errors in the location of the Venus limb on the detector. Some of the observed variance may also be caused by real differences in the feature velocities. The large planetary-scale markings move up to 25 m $s^{-1}$ faster than the smaller markings at low latitudes, producing two distinct velocity profiles. Small, slow-moving markings dominated low latitudes on the day of the Galileo encounter.

To determine the horizontal distribution of wet and dry regions in the deep atmosphere of Venus, we constructed "water maps" from ratios of narrow-band NIR images taken at wavelengths in and out of water vapor absorption bands. Differences in the water vapor abundance as large as those reported by Bell *et al.* would appear as factor of 2 intensity variations in these ratio maps. The first maps were constructed from 2.40-μm (in-band) and 2.24-μm (out-of-band) images taken at the Palomar 5-m telescope on 9 February. These maps, which were made 11 days after the observations described by Bell *et al.*, showed no evidence for enhanced water vapor mixing ratios near the bright spot. That apparent water vapor anomaly may have been dispersed beyond our detection limits by the strong vertical shears in the east-west winds below the cloud base (*21*). These ratio maps, and others compiled from ratios of 2.4-μm (in-band) and 2.3-μm (out-of-band) images taken at the 3.9-m Anglo-Australian Telescope (AAT) on 13 February (*15*), rarely show horizontal intensity contrasts larger than a few percent. Numerical simulations of these data (*15*) show that the prevailing water vapor mixing ratio is near 40 ± 20 ppmv below the clouds. These observations provide no evidence for the large, north-south water vapor gradients below the clouds that were proposed to explain the Pioneer Venus net flux radiometer measurements (*22*).

In contrast to the lower latitudes, which show bright and dark markings with a variety of spatial scales, mid-latitudes (40° to 60°) of both hemispheres were occupied by bright quasi-zonal bands. Similar structures were seen in all earlier observations (*1–3*). The absence of distinct markings frustrated efforts to track east-west velocities at these latitudes, but these bright bands may still constrain the dynamics of the middle and lower cloud decks. The reduced cloud opacity in these bands could be produced by downwelling, which transports $H_2SO_4$ droplets below the cloud base where they evaporate. The persistence of this downwelling suggests that it might be associated with the descending branch of a low-latitude cloud-level Hadley cell, like that proposed by Limaye (*23*). If this Hadley cell is confined to the region of the clouds where the NIR markings are formed, one should be able to detect it directly by measuring the north-south velocities of these markings. Unfortunately, the uncertainties in our ground-based measurements at mid-latitudes (±8 m $s^{-1}$) are too large to confirm or preclude such a cell. The higher resolution Galileo observations might provide the constraints needed to test this hypothesis.

Scattered light from the bright sunlit cusps of Venus precludes observations of night-side NIR emission in the polar regions, but the

VENUS RADIATIVE TRANSFER FOLDER

highest latitudes that can be seen (±60° to 75°) are always dark and featureless (*2*). These dark bands fall at the same latitudes as the "cold collar" seen at mid-infrared wavelengths (8 to 12 μm) (*24–26*). The cold collar has been attributed to a cold cloud top. Unlike the mid-infrared measurements, our NIR observations are not sensitive to the temperature of the cloud top. Instead, they indicate that the clouds have greater optical depths at these latitudes. The mechanisms that make the clouds more opaque and cloud tops colder at these latitudes are not currently known, but both phenomena could be produced by strong vertical convective mixing within the middle and upper cloud layers (49 to 57 and 58 to 65 km, respectively). This mixing would suspend larger cloud particles that are more opaque at NIR wavelengths. The almost adiabatic vertical temperature gradients derived from Pioneer Venus radio occultation observations at these altitudes and latitudes (*27*) appear to support this hypothesis.

The largest markings (>2000 km) at latitudes less than ±60°, including the planetary-scale dark cloud, the bright spot seen on 29 January and 10 February, and distinct features within the persistent mid-latitude bright bands (±40° to 60°) rotate from east to west in almost solid-body rotation with periods near 5.5 ± 0.15 days (Fig. 4). This corresponds to an equatorial velocity of 80 ± 3 m $s^{-1}$ (*17*), which is about 10 m $s^{-1}$ faster than that derived from earlier studies of NIR markings (*1–3*). Similar rotation periods were derived from markings tracked over both short (3- to 5-hour) and long (5- to 46-day) intervals. Unlike the largest markings, most small-scale (400 to 2000 km) markings at low latitudes had east-west velocities near 60 ± 7 m $s^{-1}$, indicating rotation periods near 7.4 ± 1 days. During the Galileo encounter, slow-moving, small-scale markings dominated the Venus night side at low latitudes (±30°), while faster moving large-scale features occupied higher latitudes.

The apparent coexistence of distinct rotation periods for large- and small-scale markings suggests that they are related to different phenomena. For example, they may provide independent estimates of the winds in the middle and lower cloud layers. To determine the plausibility of this hypothesis, we used the thermal wind equation (*28*) to estimate the north-south temperature gradient at 30° latitude implied by the observed velocity difference. If the faster component (75 m $s^{-1}$) was centered near 0.6 bar (middle cloud) and the slower component (60 m $s^{-1}$) was centered near 1.3 bars (lower cloud), the computed poleward temperature gradient is −0.14 K per degree of latitude. Measurements by the Pioneer Venus entry probes (*29*) and radio occultation experiment (*27*) reveal similar horizontal temperature gradients near the 1-bar (50 km) level and support this interpretation of the distinct NIR marking velocity profiles.


REFERENCES AND NOTES

1. D. A. Allen and J. W. Crawford, *Nature* **307**, 222 (1984).
2. D. Crisp *et al.*, *Science* **246**, 506 (1989).
3. D. A. Allen, *Icarus* **69**, 221 (1986).
4. L. W. Kamp, F. W. Taylor, S. B. Calcutt, *Nature* **336**, 360 (1988).
5. L. W. Kamp and F. W. Taylor, *Icarus* **86**, 510 (1990).
6. B. Bezard *et al.*, *Nature* **345**, 508 (1990).
7. J. H. Hoffman *et al.*, *J. Geophys. Res.* **85**, 7882 (1980).
8. V. I. Oyama *et al.*, *ibid.*, p. 7891.
9. V. I. Moroz, in *Venus*, D. M. Hunten, L. Colin, T. M. Donahue, V. I. Moroz, Eds. (Univ. of Arizona Press, Tucson, 1983), pp. 45–68.
10. C. DeBergh *et al.*, *Science* **251**, 547 (1991).
11. J. F. Bell III *et al.*, *Bull. Am. Astron. Soc.* **22**, 1052 (1990).
12. J. F. Bell III *et al.*, *Science* **252**, 1293 (1991).
13. R. Carlson *et al.*, *ibid.* **253**, 1541 (1991).
14. D. Allen, *Int. Astron. Union Circ.* 4962 (1990); D. Crisp *et al.*, *Bull. Am. Astron. Soc.* **22**, 1053 (1990).
15. D. Crisp *et al.*, *Science* **253**, 1263.
16. In January, images were taken from Cerro Tololo and Kitt Peak. In February, images were taken from Las Campanas, Kitt Peak, Palomar, Mauna Kea, and the Anglo-Australian Observatory.
17. Three different methods were used to track NIR markings. In the first, maps created from images taken at different times were displayed and the latitudes and longitudes of common markings were recorded. Displacements of markings were converted to distances and we computed velocities by dividing these values by the elapsed time. In the second method, a single map was displayed, and we selected a specific marking by surrounding it with a box. We located this feature on subsequent maps by translating the maps in latitude and longitude until the mean contrast and root-mean-square intensity difference within the chosen box were minimized. The last method was a completely automated version of the second, which used the brightness variance within specified latitude-longitude bins to track distinct markings.
18. D. Crisp, *Icarus* **77**, 391 (1989).
19. V. M. Linkin *et al.*, *Science* **231**, 1420 (1986).
20. D. Crisp *et al.*, *Adv. Space Res.* **10**, 109 (1990).
21. C. C. Counselman *et al.*, *J. Geophys. Res.* **85**, 8026 (1980).
22. H. E. Revercombe *et al.*, *Icarus* **61**, 521 (1985).
23. S. S. Limaye, *Adv. Space Res.* **5**, 51 (1985).
24. D. Diner *et al.*, *Icarus* **27**, 191 (1976); D. Diner *et al.*, *ibid.* **52**, 301 (1982).
25. F. W. Taylor *et al.*, *J. Geophys. Res.* **85**, 7963 (1980).
26. G. S. Orton, J. Caldwell, A. J. Friedson, T. Z. Martin, *Science* **253**, 1536 (1991).
27. A. J. Kliore and I. R. Patel, *J. Geophys. Res.* **85**, 7957 (1980).
28. C. B. Leovy, *J. Atmos. Sci.* **30**, 1217 (1973).
29. A. Seiff, *J. Geophys. Res.* **85**, 7903 (1980).


30. This work was funded in part by grants from the NASA Planetary Astronomy and Planetary Atmospheres Programs to the Jet Propulsion Laboratory (JPL), California Institute of Technology, and the NASA Ames Research Center. Additional support for S. McMuldroch was provided by the Science and Engineering Research Council. Computer time was provided by the Wide-Field/Planetary Camera II Project at JPL. Contribution 5067 from the Division of Geological and Planetary Sciences, California Institute of Technology.

3 April 1991; accepted 17 July 1991


# Galileo Infrared Imaging Spectroscopy Measurements at Venus


R. W. CARLSON, K. H. BAINES, TH. ENCRENAZ, F. W. TAYLOR, P. DROSSART, L. W. KAMP, J. B. POLLACK, E. LELLOUCH, A. D. COLLARD, S. B. CALCUTT, D. GRINSPOON,* P. R. WEISSMAN, W. D. SMYTHE, A. C. OCAMPO, G. E. DANIELSON, F. P. FANALE, T. V. JOHNSON, H. H. KIEFFER, D. L. MATSON, T. B. MCCORD, L. A. SODERBLOM



**During the 1990 Galileo Venus flyby, the Near Infrared Mapping Spectrometer investigated the night-side atmosphere of Venus in the spectral range 0.7 to 5.2 micrometers. Multispectral images at high spatial resolution indicate substantial cloud opacity variations in the lower cloud levels, centered at 50 kilometers altitude. Zonal and meridional winds were derived for this level and are consistent with motion of the upper branch of a Hadley cell. Northern and southern hemisphere clouds appear to be markedly different. Spectral profiles were used to derive lower atmosphere abundances of water vapor and other species.**


THE FEBRUARY 1990 GALILEO FLYBY provided a unique opportunity to investigate the clouds, motions, and deep-atmosphere composition of Venus with infrared imaging spectroscopy. The spectral range and spatial resolution of the


R. W. Carlson, K. H. Baines, L. W. Kamp, P. R. Weissman, W. D. Smythe, A. C. Ocampo, T. V. Johnson, D. L. Matson, Jet Propulsion Laboratory, California Institute of Technology, Pasadena, CA 91109.
Th. Encrenaz, P. Drossart, E. Lellouch, Observatoire de Paris, F-92195 Meudon, France.
F. W. Taylor, A. D. Collard, S. B. Calcutt, Oxford University, Oxford OX1 3PU, United Kingdom.
J. B. Pollack and D. Grinspoon, National Aeronautics and Space Administration (NASA) Ames Research Center Moffett Field, CA 94035.
G. E. Danielson, Division of Geological and Planetary Sciences, California Institute of Technology, Pasadena, CA 91109.
F. P. Fanale and T. B. McCord, University of Hawaii, Honolulu, HI 96822.
H. H. Kieffer and L. A. Soderblom, U.S. Geological Survey, Flagstaff, AZ 86001.

*Present address: University of Colorado, Boulder, CO 80309.